PREDICTION OF ASH DEPOSITION IN A PULVERIZED COAL-FIRED UTILITY BOILER

Rafaela Frota Reinaldo
Universidade Federal de Santa Catarina, Departamento de Engenharia Mecânica
Laboratório de Combustão e Engenharia de Sistemas Térmicos
88.040-900, Florianópolis – SC, Brazil
rafaela@cet.ufsc.br

Edson Bazzo
Universidade Federal de Santa Catarina, Departamento de Engenharia Mecânica
Laboratório de Combustão e Engenharia de Sistemas Térmicos
88.040-900, Florianópolis – SC, Brazil
ebazzo@emc.ufsc.br

João Luis Toste de Azevedo
Instituto Superior Tecnico, Departamento de Engenharia Mecânica
Av. Rovisco Pais, 1049-001 Lisboa, Portugal
toste@navier.ist.utl.pt

Abstract. *The ash deposition on heat transfer surfaces of utility boilers is one of the main problems associated to the use of coal. The ash deposits reduce the heat transfer in the boiler, causing a decrease of the boiler efficiency. The prediction of ash deposition gives important information to boilers' designers and operators. This work presents numerical simulation of the flow, heat transfer and combustion in a pulverized coal furnace in order to predict the ash deposition in the furnace walls and superheater tubes. The ash deposition model is based on the concepts of impact efficiency and sticking probability of the particles. This calculation procedure is an extension of the Computational Fluid Dynamics based model for pulverized coal combustion already extensively used at Instituto Superior Tecnico. Further works concerning ash deposition measurements will be carried out for chemical characterization of the ash deposits and comparison with the predicted results.*

Keywords*. utility boiler, ash deposition, computational fluid dynamics, pulverized coal.*

1. Introduction

The computational fluid dynamics codes for pulverized coal combustion have an essential importance in the analysis of utility boilers performance. Important parameters that can be analysed using the numerical model are gas mixing, heat transfer, particulate matter combustion, NO_x formation, and particulate trajectories (Coimbra et al., 1994).

Nowadays, 90% of the word-wide primary energy is produced by the use of fossil fuels: oil, natural gas and coal (Tissot, 2001). Despite the other alternatives for the use of these fuels, the projections show that they will continue to supply the expanding energy demand (Smoot, 1993). Coal is the most abundant fossil fuel in the world as illustrated in table 1 and will assume an important role in the electricity production. The three major coal combustion techniques are: suspension firing, grate firing, and fluidized bed combustion. Suspension firing is the technique employed in pulverized coal furnaces, which are used in high capacity utility boilers.

Efficiency and trustworthiness are fundamental on the operation of pulverized coal power plant units. The ash deposition on heat transfer surfaces of utility boilers is one of the main problems associated to the use of coal. The low thermal conductivity of the ash deposits reduces the heat transfer in the boiler, causing a decrease of the boiler efficiency. The excessive use of the sootblowers causes erosion in the tubes and in a limiting case can cause tube failure. On the other hand, the restrained use of sootblowers takes to a critical situation where the sootblowers are not able to remove the fouling deposits and it is necessary to shutdown the boiler in order to clean it. The prediction of the ash deposition rate can provide the information as to the frequency of soot blowing to the boiler's operator (Smoot, 1992).

Table 1 - 2002 World Energy Reserves, in thousand million (10^9) tons of oil equivalent (Gtoe)

Fuel	Proved reserves (10^9 Gtoe)	Production (per year)
Coal*	659.6	2.4
Oil	142.7	3.6
Natural Gas**	143.0	2.3

Source: BP Amoco Statistical Review of World Energy, 2003.
* 1 tonne of coal = 0.67 tonne of oil equivalent (approximately)
** 1 trillion cubic feet of natural gas = 26 million tonnes of oil (approximately)

2. Description of the problem

The utility boiler analysed on this work produces superheated and reheated steam for a 125MWe capacity generator and consists of a natural circulation system with external downcomers and tube wall membranes connected to the same boiler drum. The furnace is front wall fired with sixteen burners divided in four rows corresponding to four pulverised coal mills. Each wall burner consists of several concentric inlets with two main annulus inlets, the inner inlet with 0.50m diameter feeds coal transported by primary air, surrounded by another annulus with 1.02m for secondary air. The combustion gases flow upwards in the furnace and after the boiler arch through the final superheater and reheaters, which are located in the exit of the combustion chamber. Then the gases flow down through the primary superheater, secondary superheater and economizer that are located in the convection chamber. The final superheater is composed of 40 panels with transversal pitch of 300mm. Each panel has seven tubes in the flow direction with external diameter equal to 31.8 mm and 60mm pitch. The location of the final superheater is presented in Fig. (1).

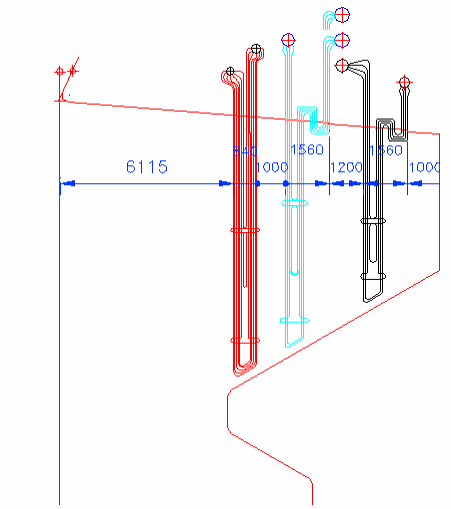

Figure 1. Final superheater and reheaters locations.

Figure (2) shows a typical ash deposit on the final superheater tubes. It is observed that the ash deposit is localized on the front side of the tube, that is, on the side facing the flow. This type of configuration is a characteristic of an inertial impact deposition. The composition of the coal is characterized by its ultimate analysis, presented in the Tab. (2). The corresponding volatile matter is approximately 20.9%. The fly ash composition is presented in Tab. (3).

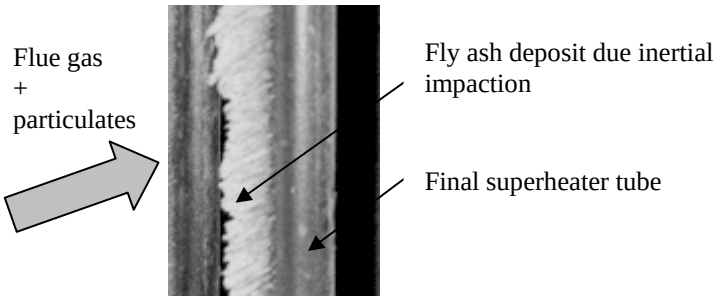

Figure 2. Ash deposit at the superheater tube (Courtesy of Tractebel Energia)

Table 2 –Ultimate coal composition

	%
Inorganic matter	37.0
Moisture	10.0
Carbon	43.04
Hydrogen	2.87
Sulphur	2.87
Oxygen + nitrogen	4.22

Source: Tractebel Energia

Table 3 – Fly ash composition

	%
SiO_2	57.93
Al_2O_3	27.47
Fe_2O_3	5.97
K_2O	2.80
CaO	2.03
TiO_2	1.40
MgO	0.90
Na_2O	0.37
MnO	0.073
Fire Loss	0.22
Total	99.22

Source: Tractebel Energia, 2000

The granulometric analysis of the coal was made using a sieving classifier, with mesh 200, 100, 60 and 20 corresponding to openings equal to 0.074, 0.147, 0.246 and 0.833 mm respectively. The granulometric analysis of the fly ash was made by laser diffractometry (Tractebel Energia, 2000). The size distributions of the coal and fly ash are presented in Fig. (3).

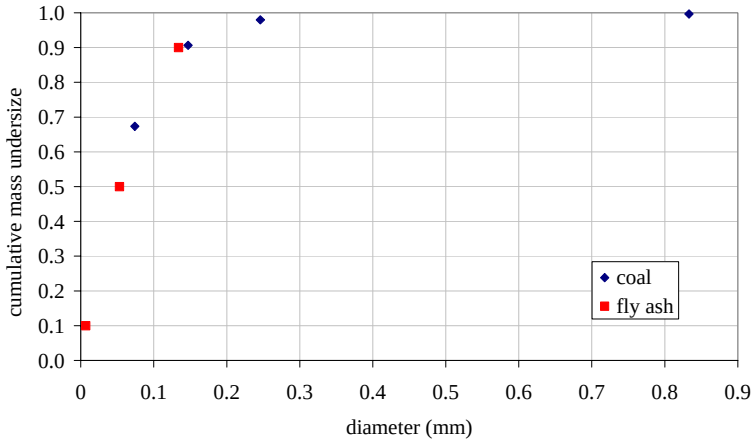

Figure 3. Coal and fly ash granulometric distributions

It can be observed in Fig. (3) that the fly ash distribution is similar to the coal distribution. The size distributions of the pulverized coal and fly ash can be represented by a Rosin-Rammler function, given by Eq. (1)

$$F(D) = 1 - \exp\left(-\frac{D^n}{D_r^n}\right) \qquad (1)$$

where F(D) is the cumulative mass undersize, D_r the mean diameter and n the exponential parameter, presented in Tab.(4).

Table 4 – Rosin-Rammler parameters

	Coal	Fly Ash
D_r (mm)	0.0658	0.0654
n	1.05	1.01

The values of the mean diameter and the exponential parameter of both distributions are very close, that confirms the similarity between the size distributions. Based on this fact, it is assumed that one coal particle burns becoming one ash particle of equal diameter, considering the hypothesis that inorganic matter structure remains unaffected during carbon conversion.

3. Methodology

3.1. Numerical Model

The numerical model of the combustion chamber is based on the turbulent flow calculation using balance equations for mass, momentum components and turbulence quantities: turbulent energy and its dissipation. All the balances for the continuum gas phase are performed in an Eulerian base using a similar discretisation procedure, except for the continuity equation that is treated by the Simple algorithm to calculate pressure. Gaseous combustion is modelled using the mixture fraction and its variance based on a clipped Gaussian distribution. The combustible gases are considered as a result of the particle phase devolatilization and char combustion. Gas enthalpy is calculated from an energy balance, considering the heat exchanged by radiation based on the discrete transfer method and the heat exchanged with the particles. Temperature is calculated based on the average enthalpy thus obtained and on the gas composition calculated with the mixture fraction and its variance. The particles trajectories are simulated using a Lagrangian approach, where representative particles are tracked in the flow domain calculating their temperature and mass evolution, with the aid of semi-empirical models. More details of the general approach of pulverized coal boilers models are reported by Toledo and Azevedo (2003). In the region of the final superheater and reheater an energy sink term is calculated taking into account the convection and the radiation heat transfer from the combustion gases to the surface of the tube. Details of the calculation are presented in the work of Reinaldo et al. (2003).

A numerical simulation was performed considering the standard operation condition of 125MWe, with the 1st, 2nd and 3rd rows of burners operating with 23.3 kg/s of pulverized coal with 164.8 kg/s of air. At this operation condition the steam production is 395 ton/h at 788K. The pressure is 121.6 bar in the final superheater and 27.5 bar in the reheater. Two swirl burners' arrangements have been simulated, and are denoted by case A and case B as shown in Fig. (4), items (a) and (b), respectively. Three scenarios were considered for analysis in order to show the influence of the primary air velocity on the particle deposition. In scenarios 1, 2 and 3 the primary air velocities are fixed 0, 9.78 and 19.60 m/s as boundary condition, respectively. The primary air flow remains constant and only the boundary conditions change.

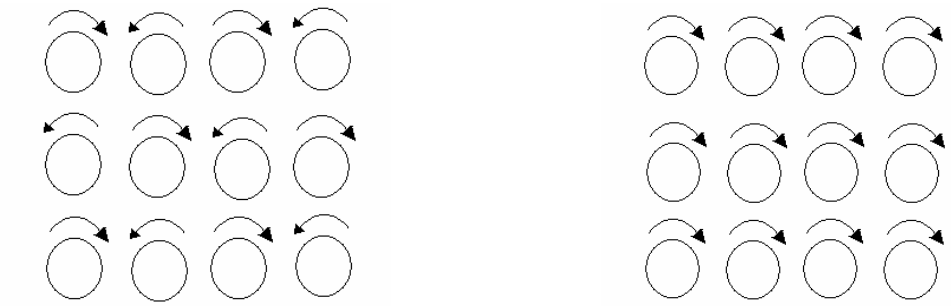

(a) case A (b) case B

Figure 4. Swirl burners' arrangements.

The numerical results are obtained using a non-uniform grid of 40 x 69 x 129 cells for the flow calculations, with finer grids in the burners' zone, and uniform grid of 17 x 12x 40 cells for the radiation heat transfer calculation. About 5000 iterations were required to achieve a converged solution.

3.2. Particle tracking

The momentum and energy balance to the particle are performed along representative particle trajectories, considering instantaneous gas velocities calculated from a stochastic model. Empirical models are used to describe coal particle devolatilisation and char combustion in sequence.

The particles trajectories are calculated solving the motion equation of a particle immersed in a continuum phase, taking into account the drag and gravitational forces, as expressed by Eq. (2),

$$\frac{d\vec{u}_p}{dt} = \frac{3}{4}\frac{\rho_g}{\rho_p}\frac{C_D}{d_p}\left|\vec{u}_g - \vec{u}_p\right|\left(\vec{u}_g - \vec{u}_p\right) + \vec{g} \qquad (2)$$

where $\overrightarrow{u_p}$ and $\overrightarrow{u_g}$ are the particle and the gas velocities, respectively, ρ_p and ρ_g are the particle and the gas densities, respectively, d_p is the particle diameter, $\vec{g}$ is the gravitational acceleration and C_D is the particle drag coefficient given by,

$$C_D = 24\left(1 + 0.15\,\mathrm{Re}_p^{\,0,687}\right)/\mathrm{Re}_p \qquad (3)$$

where Re_p is the particle Reynolds number as function of the relative particle/gas velocity modulus.

The particle trajectories are calculated every 10 flow iterations. The particle tracking is made taking into account 10 particle sizes with 4 start locations per particle inlet and 30 particle trajectories per start location.

3.3. Particle deposition model

The relative importance of the mechanisms that control the transport of particles to a surface depends, mainly, of the particle size. Molecular diffusion and thermophoresis are dominant for very small particles (<1μm), and the inertial impaction is dominant for large particles (>10μm). According to the work of Kær et al. (2001) the order of magnitude concerning the deposition rate controlled by the inertial impaction is greater then that controlled by the others mechanisms. Taking into account this statement, the present work considers only the inlet impaction mechanism. At this condition, the rate of ash deposition in a surface depends on the total mass flux of particle, the parcel of particles that will impact and their tendency to stick on the surface, as expresses by Eq. (4),

$$I = q\,\eta_I\,\eta_C \qquad (4)$$

where I is the rate of ash deposition, q is the mass flux of particles in the flow, η_I is the impact efficiency and η_C is the sticking probability. In this work the geometry change due to ash deposition is not considered.

For a flow passing by a cylinder, the inertial impaction depends whether particles follow the gas streamlines or depart from them, and is function of the inertial force and the drag force acting in a particle. The Stokes number represents the ratio between these two forces.

$$St \equiv \frac{\rho_p d_p^2 v_p}{9\mu_g D_c} \qquad (5)$$

where v_p is the particle velocity modulus, μ_g is the gas viscosity and D_c is the cylinder diameter. For low Stokes number the particle follow the streamlines and will not collide in an obstacle. For high Stokes number the particle is hardly affected by the gas streamline and will collide with the obstacle. As considered by Huang et al. (1996), the impact efficiency is determined as a function of Stokes number, according to Eq. (6)

$$\eta_I = \left[1 + b(St-a)^{-1} + c(St-a)^{-2} + d(St-a)^{-3}\right]^{-1} \qquad (6)$$

where a = 0.125, b = 1.25, c = 0.014 and d = 0.508 x 10^{-4}.

The sticking probability is the ratio of the particles that stick on the surface after the collision, and is a function of the critical and particle viscosities. The sticking probability of a particle with viscosity smaller than the critical viscosity is 100%. If the particle viscosity is greater than the critical value, the sticking probability is equal to the ratio between the critical and particle viscosities, as expressed by the Eq. (7),

$$\eta_C = \begin{cases} \dfrac{\mu_{crit}}{\mu} & \text{if } \mu > \mu_{crit} \\ 1 & \text{if } \mu \le \mu_{crit} \end{cases} \qquad (7)$$

where μ_{crit} and μ are the critical and particle viscosities respectively. The value of the critical viscosity is considered equal to 10^4Pa.s. Again, following the methodology used by Huang et al. (1996), the particle viscosity is a function of the composition and temperature, T in Kelvin, given by the following expression,

$$\log_{10}(10\mu) = \frac{10^7\,\mathrm{m}}{(\mathrm{T}-150)^2} + \mathrm{c} \qquad (8)$$

where m and c are defined by the equations (9) and (10), respectively

$$m = 0.00835[SiO_2] + 0.00601[Al_2O_3] - 0.109 \quad (9)$$

$$c = 0.0415[SiO_2] + 0.0192[Al_2O_3] + 0.0276[Fe_2O_3] + 0.016[CaO] - 3.92 \quad (10)$$

as a function of the mass fractions, in percentage, of the ash constituents.

4. Results

The velocity and the gas temperature fields, for scenarios 1 and 3, in a vertical plane crossing the first column of burners from the right side are presented in Fig. (5) and Fig (6), respectively. The flow is characterized by the formation of a large recirculation zone at the ash pit region and a deflection of the flow from the burners at the rear wall of the furnace. This leads to higher velocities close to the furnace arch where the flow is deflected towards the superheater panels. The location of the main flame region can be identified from the temperature field. Larger temperatures are observed at the core of the furnace, where most volatiles are burned. The gases are then cooled when deflected towards the furnace exit. It is clear, that the flame is longer and thinner in scenario 3 than in scenario 1, touching the rear furnace wall. The shown results correspond to the swirl arrangement B, that is the actual operating condition of the furnace.

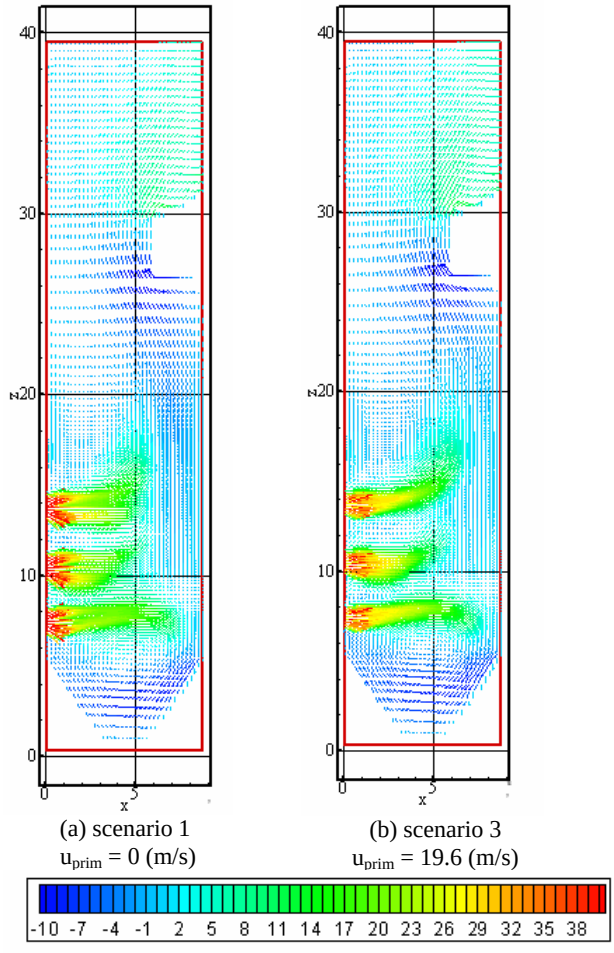

(a) scenario 1 u_{prim} = 0 (m/s) (b) scenario 3 u_{prim} = 19.6 (m/s)

Figure 5. Gas velocity in the furnace

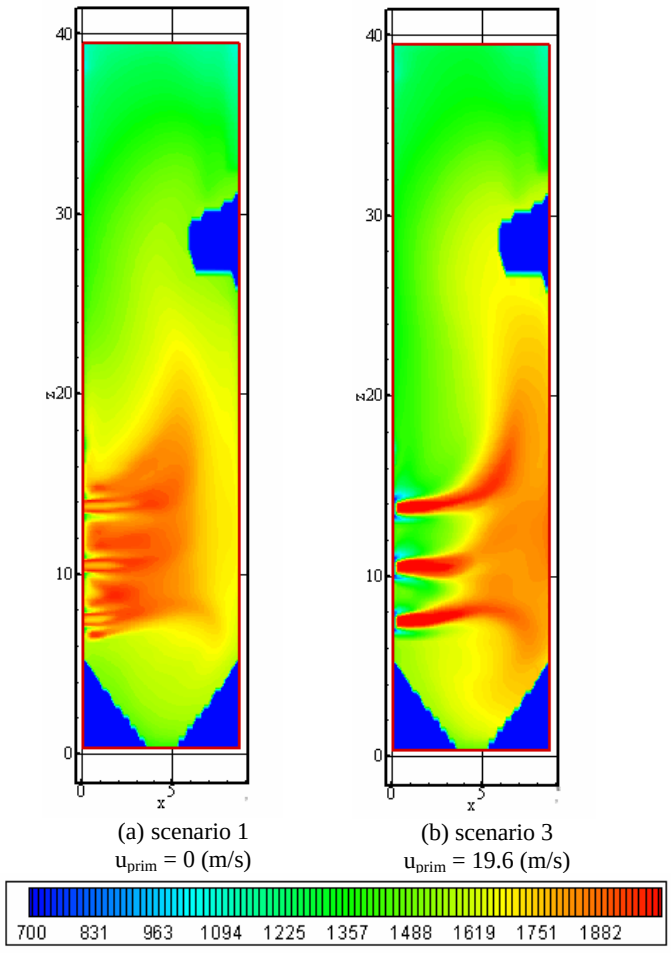

(a) scenario 1 u_{prim} = 0 (m/s) (b) scenario 3 u_{prim} = 19.6 (m/s)

Figure 6. Gas temperature in the furnace

For case B and scenario 1, the particles deposition map in the front, right, rear and left side of the furnace walls is presented in Fig. (7), items (a), (b), (c) and (d), respectively. It can be observed in Fig. (7) (a) that the particle deposition in the front wall is more concentrated in the region between the 2nd and 3rd rows of burners. In the rear wall the particle deposition is more concentrated in the region in front of the burners, in the top right side, as can be observed in Fig (7) (c). It can be also observed in the rear wall that the particle deposition is also very intense in the region below the furnace arch. The particle deposition in the left wall, Fig. (7)(d), is more concentrated in the middle of region bellow the furnace arch. In the right wall, Fig. (7) (b), the particle deposition is more dispersed than in the right wall. Higher particle impact concentration can be observed in the middle region bellow the furnace arch as well in the middle of region above the furnace arch. A deposition in the front part of the ash pit region is also observed. For case B and scenarios 2 and 3, the particles deposition maps are presented in Fig. (8) and Fig. (9), respectively.

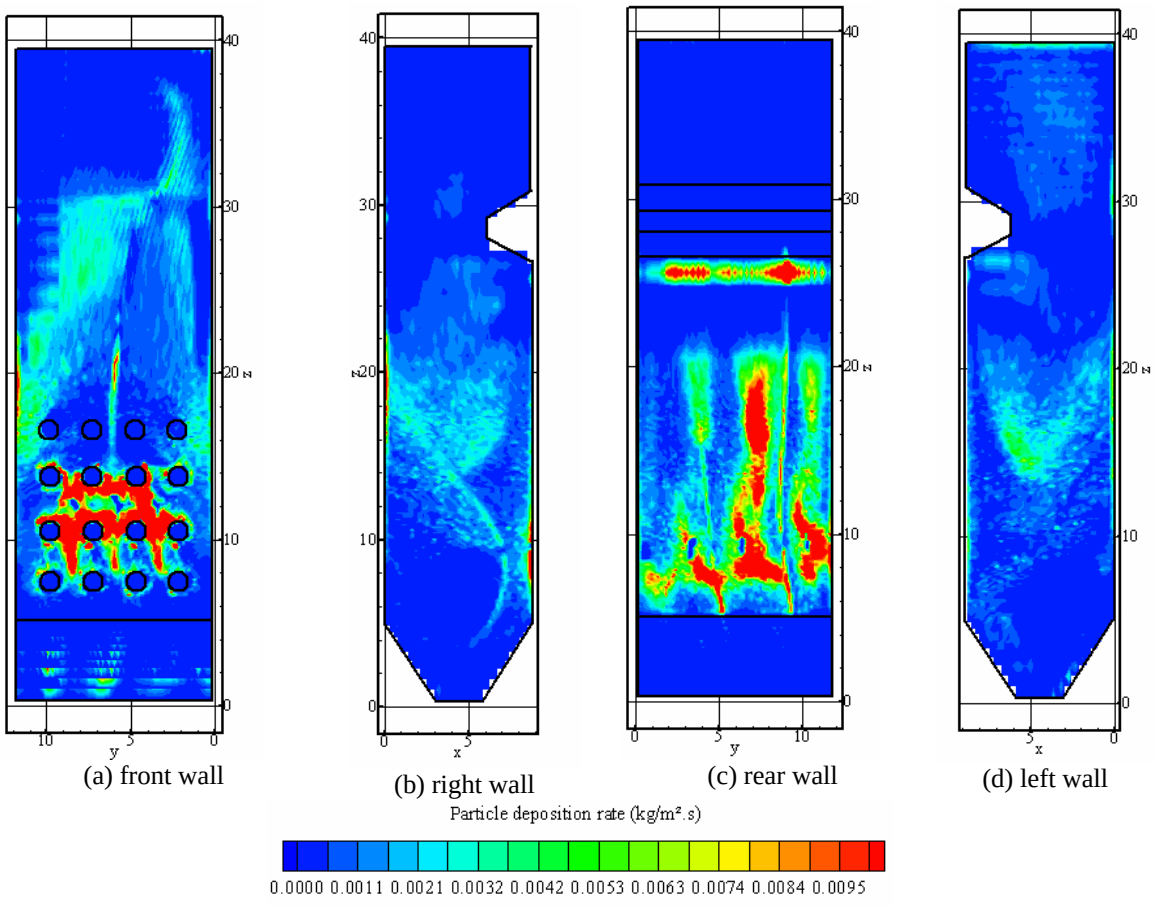

(a) front wall (b) right wall (c) rear wall (d) left wall

Figure 7. Particle wall deposition map – scenario 1

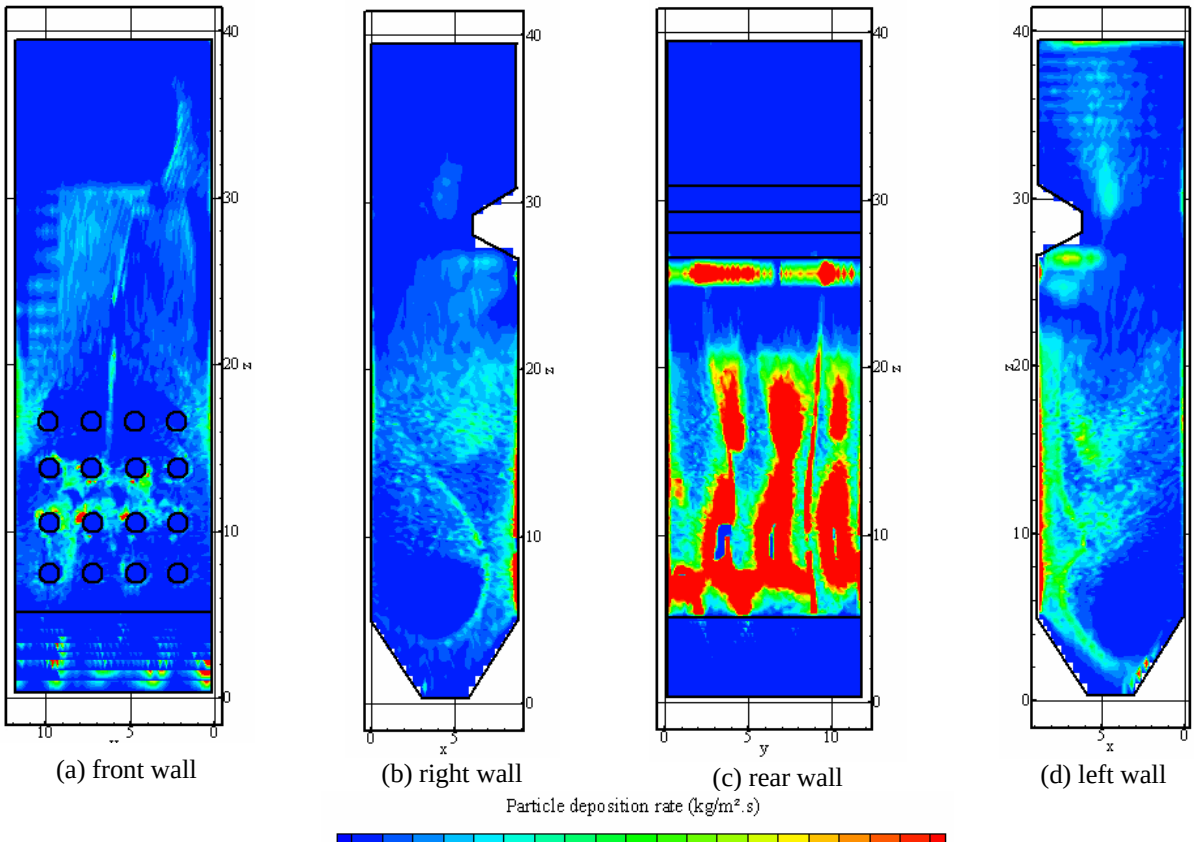

(a) front wall (b) right wall (c) rear wall (d) left wall

Figure 8. Particle wall deposition map– scenario 2

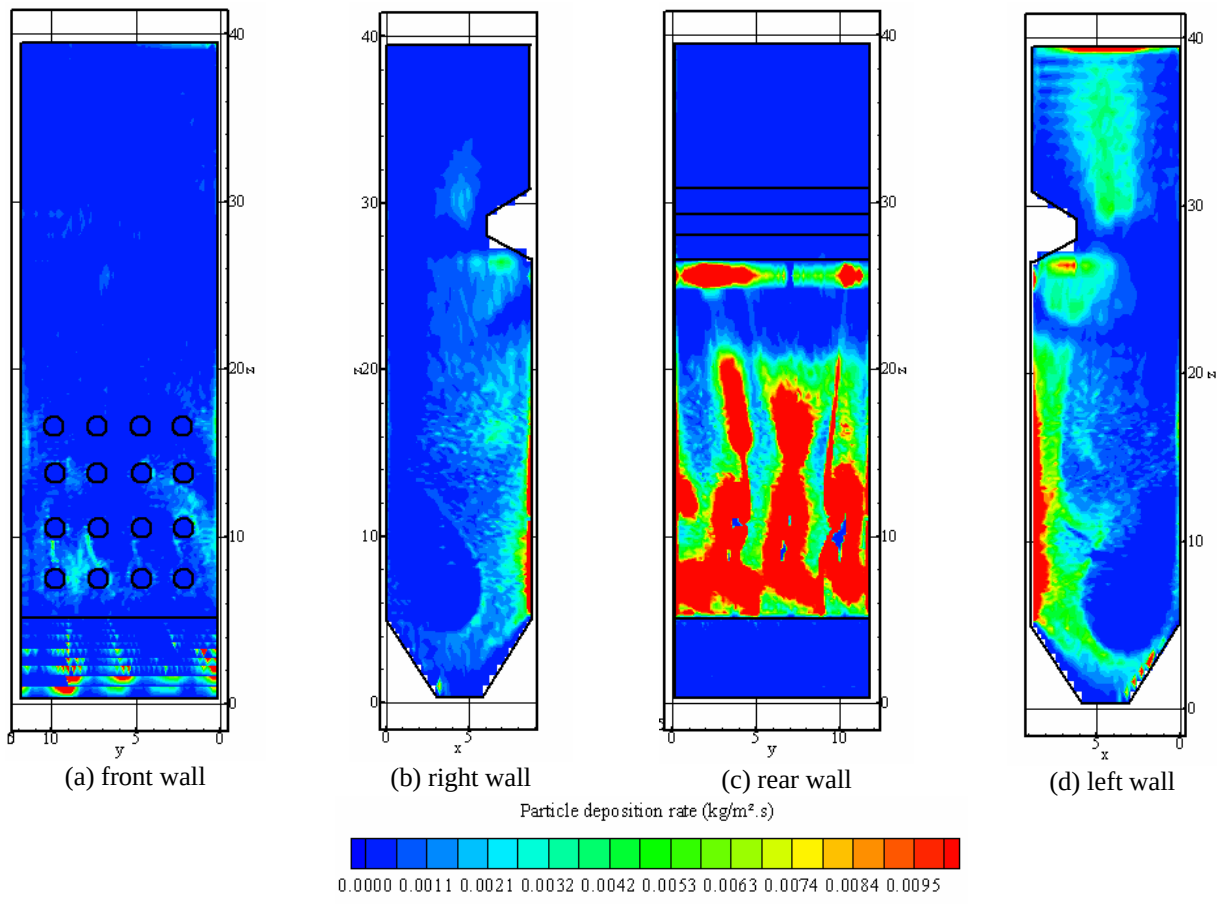

Figure 9. Particle wall deposition map – scenario 3

One can observe the strong influence of the primary air velocity boundary condition on the ash deposition at the furnace walls. The increasing of the primary air velocity increases the particles deposition rate at the rear and side walls. By the same way, it decreases the particle deposition at the front wall (see Fig. (7), Fig. (8) and Fig.(9)).

In Table (5) it is shown a summary of the numerical results concerning to particle collision and deposition on the furnace walls and final superheater, for scenarios 1, 2 and 3, and also for both swirl arrangements, cases A and B . In general, it was observed that:

i) the particles collision and deposition at the furnace walls increase with the increasing in the primary air inlet velocity;
ii) the total stick probability increases from 45 to 70% when the primary air inlet velocity increases from 0 to 19.60 m/s;
iii) the particles flow across the bundle tubes and the ash deposition at the final superheater decrease, as a consequence of the increasing in the primary air velocity;
iv) about 30% of the particles crossing the superheater stick on it;
v) the swirl arrangement has little influence on the global results.

Table 5 – Particle mass flow and deposition for A and B swirl arrangements

Case	Primary air inlet u (m/s)	Total inorganic matter (kg/s)	Collide at the walls (kg/s)	Stick on the walls (kg/s)	Cross the final superheater (kg/s)	Stick on the final superheater (kg/s)
A	0.0	8.62	4.90	2.29	3.54	1.01
B	0.0		4.72	2.18	3.69	1.05
B	9.78		5.37	3.21	2.80	0.78
B	19.60		6.53	4.58	1.57	0.50

For scenario1, the particle deposition map at the inlet superheater region is presented in Fig. (10) (a) and (b), corresponding to case A and case B, respectively. In the case A, Fig. (10) (a), a high particle deposition rate is observed on the center of the plane stretching up towards the top and right and left corners. In the case B, Fig. (10) (b), a high deposition rate is observed on the center of the plane stretching towards up right corner. It can be also observed a significative deposition on the left and top sides.

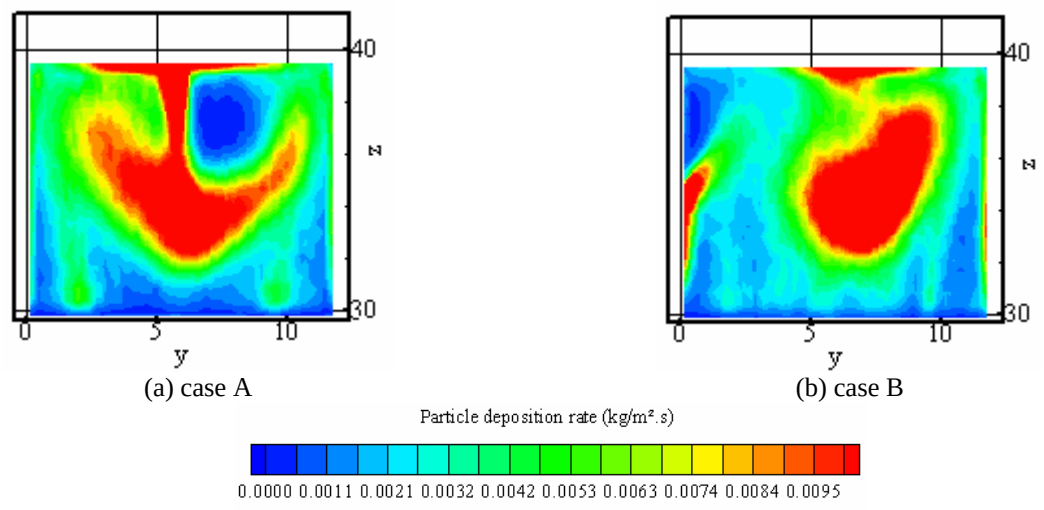

(a) case A (b) case B

Figure 10. Particle deposition map

5. Conclusions

A CFD based methodology to predict the ash deposition rate in the furnace and tube walls is presented. The total sticking probability along the furnace walls increases with the increasing in the primary inlet air velocity. The total ash deposition is less dependent of the burners swirl arrangements. However, its influence on the local deposition is very strong, either on the furnace walls as on the final superheater tubes. The particles deposition on the final superheater tube is more concentrated at the center, and about 30% of the particles that cross the superheater stick on it. Further work concerning ash deposition measurements will be carried out for comparison with the predicted results. The influence of the deposits distribution on the heat transfer to the walls should also be addressed in future.

6. References

BP Amoco, 2003, Statistical Review of World Energy.

Coelho, P. J., 1999a, "Mathematical Modelling of the Convection Chamber of a Utility Boiler", Numerical Heat Transfer, Part A, Applications, Vol. 36(4), pp.411-428.

Coimbra, C.F.M., Azevedo, J.L.T. and Carvalho, M.G., 1994, "3-D Numerical Model for Predicting NOx Emissions from a Pulverised Coal Industrial Boiler", FUEL, 73(7): 1128-1134.

Kær, S.K., M., Rosendahl, L. and Adamsen, P., 2001, "A Particle Deposition Model Applicable to Full-Scale Boiler Simulations: Sub-Model Testing", Proceedings of FEDSM'01, New Orleans, Louisiana, May 29-June 1, 2001.

Huang, L.Y., Norman, J.S., Pourkashanian, M., e Williams, A., 1996, "Prediction of Ash Deposition on Superheater Tubes from Pulverized Coal Combustion", Fuel, vol. 75, pp. 271-279

Reinaldo, R. F., Azevedo, J.L.T., Bazzo, E., 2003, "Use of a CDF Based Numerical Model to Calculate Heat Transfer in Boiler Superheaters Panels", Proceedings of the 17th International Congress of Mechanical Engineering, São Paulo, Brazil.

Smoot, L.D., 1992, "Fundamentals of Coal Combustion: For Clean and Efficient Use", Coal Science and Technology, Vol. 20.

Smoot, L.D., 1993, "Role of Combustion Research in the Fossil Energy Industry", Energy &Fuels, Vol. 7, pp. 689-699.

Tissot, B., 2001, "Quel avenir pour les combustibles fossiles? Les avancées scientifiques et technologiques permettront-elles la poursuite d'un développement soutenable avec les énergies carbonées ? ", C.R. Acad. Sci. Paris, Sciences de la Terre et des planètes, Vol. 333, pp. 787-796.

Toledo, R., and Azevedo, J.L.T., 2003, "CDF Based Numerical Modeling of Different Furnace Configurations Using Air Staging and Reburning", Proceedings of the 17th International Congress of Mechanical Engineering, São Paulo, Brazil.

Tractebel Energia, 2000, "Caracterização das cinzas pesadas e leves geradas nas usinas termelétricas do complexo Jorge Lacerda , em Capivari de Baixo/SC", Internal Report, Universidade Federal do Rio Grande do Sul – Departamento de Materiais.

7. Aknowledgements

The authors thank CAPES and CNPq for providing a scholarship to R. F. Reinaldo, and CAPES and GRICES for the financial support to the international cooperation program between the Federal University of Santa Catarina (Brazil) and the Instituto Superior Tecnico (Portugal).